Available online at www.sciencedirect.com
ScienceDirect
Materials Science and Engineering C 27 (2007) 1222 – 1226
MATERIALS SCIENCE & ENGINEERING C
www.elsevier.com/locate/msec

Phonons in sapphire Al_2O_3 substrate for ZnO and GaN

H.W. Kunert [a,*], A.G.J. Machatine [b], A. Hoffmann [a], G. Kaczmarczyk [a], U. Haboeck [a], J. Malherbe [b], J. Barnas [c], M.R. Wagner [a], J.D. Brink [b]

[a] *Institut für Festkörperphysik, Technische Universität Berlin, Hardenbergstr. 6, 10-623 Berlin, Germany*
[b] *Department of Physics, University of Pretoria, 0001 Pretoria, South Africa*
[c] *Department of Physics, Adam Mickiewicz University, ul. Umultowska 85, 61-614 Poznan, Poland*

Received 26 May 2006; received in revised form 15 August 2006; accepted 16 August 2006
Available online 5 October 2006

Abstract

By means of standard method of placing the vectors upon each ion in the basis (2-Al, 3-O) and acting by symmetry operators of sapphire space group onto the basis we obtain Lattice Mode Representation (LMR). The decomposition of the LMR onto irreducible representations (irrps) corresponding to the high symmetry point and lines results in symmetry allowed first order non-interacting modes originating from the entire first Brilloiun zone. First order Raman active modes are determined by symmetrized square of Kronecker products of sapphire vector representation. The selection rules for the second and third order Raman processes follow from the symmetrized Kronecker Products (square and cubes). Frequently the irrps are complex. In such cases the time reversal symmetry (TRS) must be taken into account. We have also investigated the effect of the TRS in sapphire and ZnO which leads to an extra degeneracy.

Keywords: Phonons; Sapphire; Group theory; Time reversal; Zno; GaN

1. Introduction

The lattice structure of sapphire belongs to the trigonal system (space group D^6_{3d}–$R\bar{3}c$). High quality synthetic sapphire is widely used as substrate material for solid state applications. Recent developments permit growth of heterostructures, multi-layers, and superlattices from the group-III nitrides on sapphire, and enormous progress in semiconductor research enabled fabrication of GaN-based blued emitting diodes and laser devices[1,2]. Due to the Debye frequency and mechanical isotropy, corundum is the perfect candidate for ballistic phonon experiments [3,4]. Moreover, with respect to the low absorption and incoherent cross section of both the oxygen and the aluminum ions, sapphire is a perfect candidate for inelastic scattering experiments [5–7]. Absorption by higher harmonics of the fundamental lattice vibrations (multiphonon processes) have been studied [8,9]. The present work focuses on the selection rules for multiphonon processes in sapphire, ZnO, and GaN.

2. Determination of the possible vibrational modes in Al_2O_3 with D^6_{3d} space group at $k=0$ of the first Brillouin zone

In order to derive the LMR [10], we have introduced twenty seven real basis vectors, three displacement and twenty four angles, shown in Fig. 1.

The angles in the Fig. 1 are defined as follows: $\alpha_1(312)$; α_2 (123); $\alpha_3(231)$; $\beta_1(412)$, $\beta_2(423)$, $\beta_3(431)$, $\beta_4(421)$, $\beta_5(432)$, β_6 (413); $\delta_1(140)$, $\delta_2(240)$ and $\delta_3(340)$, for the lower pyramid. The displacements are placed at the atoms (ions) of oxygen (1) d_1, (2) d_2 and (3) d_3. Similarly we define the angles for the upper pyramid with primes. The numbers refer to the ions that make angle in a clockwise manner. The upper ions are obtained through inversion at the central aluminum atom, labeled as $4=4'$. The displacements of the upper (primed displacements)

* Corresponding author.
E-mail address: hkunert@nsnper1.up.ac.za (H.W. Kunert).

0928-4931/$ - see front matter © 2006 Elsevier B.V. All rights reserved.
doi:10.1016/j.msec.2006.08.014

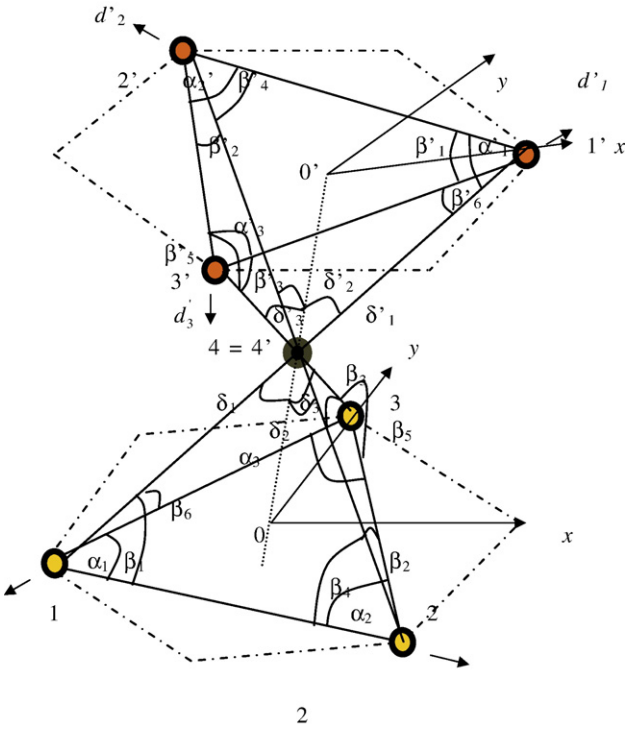

Fig. 1. Arrangement of O and Al atoms.

and lower pyramids (unprimed displacements) are related as follows:

$$d_1 = -d_1';\ d_2 = -d_2';\ d_3 = -d_3';\ \alpha_1(312) = \alpha_1'(3'1'2');\ldots\ldots;\delta_3(340) = \delta_3'(3'4'0').$$

The angles of primed coordinates are equivalent to the angles of non-primed ones. Acting by symmetry operators onto the introduced basis we obtain twelve matrices, which form the LMR. It is enough to generate LMR by three generators. For the first generator we have

$$\{C_3^+|0\}\begin{bmatrix} d_1 \\ d_2 \\ M \\ M \\ \delta_3' \end{bmatrix} = A\begin{bmatrix} d_1 \\ d_2 \\ M \\ M \\ \delta_3' \end{bmatrix}$$

where

$$A = D(\{C_3^+|0\}) = \lfloor d_2\ d_3\ d_1\ \alpha_2\ \alpha_3\ \alpha_1\ \beta_2\ \beta_3\ \beta_1\ \beta_5\ \beta_6\ \beta_4\ \delta_2\ \delta_3\ \delta_1\ \alpha_2'\ \alpha_3'\ \alpha_1'\ \beta_2'\ \beta_3'\ \beta_1'\ \beta_5'\ \beta_6'\ \beta_4'\ \delta_2'\ \delta_3'\ \delta_1'\rfloor$$

The **A** is a block matrix,

$$\mathbf{A} = \begin{bmatrix} A_1 & & \\ & O & \\ & & A_9 \end{bmatrix}, \text{with the sub-matrix } \mathbf{A}_i = \begin{bmatrix} 0 & 1 & 0 \\ 0 & 0 & 1 \\ 1 & 0 & 0 \end{bmatrix};\ (i=1,\ldots,9).$$

For the second generator we obtain

$$\left\{\sigma_{v1}|00\ \frac{1}{2}\right\}\begin{bmatrix} d_1 \\ d_2 \\ M \\ M \\ \delta_3' \end{bmatrix} = B\begin{bmatrix} d_1 \\ d_2 \\ M \\ M \\ \delta_3' \end{bmatrix}$$

with

$$B = D\left(\left\{\sigma_{v1}|00\ \frac{1}{2}\right\}\right) = \lfloor d_2\ d_3\ d_1\ \alpha_2\ \alpha_3\ \alpha_1\ \beta_2\ \beta_3\ \beta_1\ \beta_5\ \beta_6\ \beta_4\ \delta_2\ \delta_3\ \delta_1\ \alpha_2'\ \alpha_3'\ \alpha_1'\ \beta_2'\ \beta_3'\ \beta_1'\ \beta_5'\ \beta_6'\ \beta_4'\ \delta_2'\ \delta_3'\ \delta_1'\rfloor$$

Finally, for the third generator we find

$$\left\{C_2|00\ \frac{1}{2}\right\}\begin{bmatrix} d_1 \\ d_2 \\ M \\ M \\ \delta_3' \end{bmatrix} = C\begin{bmatrix} d_1 \\ d_2 \\ M \\ M \\ \delta_3' \end{bmatrix}$$

where

$$C = D\left(\left\{C_2|00\ \frac{1}{2}\right\}\right) = \lfloor d_2\ d_3\ d_1\ \alpha_2\ \alpha_3\ \alpha_1\ \beta_2\ \beta_3\ \beta_1\ \beta_5\ \beta_6\ \beta_4\ \delta_2\ \delta_3\ \delta_1\ \alpha_2'\ \alpha_3'\ \alpha_1'\ \beta_2'\ \beta_3'\ \beta_1'\ \beta_5'\ \beta_6'\ \beta_4'\ \delta_2'\ \delta_3'\ \delta_1'\rfloor$$

Proceeding in the same manner, or using multiplication tables for corundum, we obtain all the other nine matrices of LMR for sapphire. The character of the LMR together with the characters of irrps (at $\boldsymbol{k}=0$) [11] of Al_2O_3 are given in the Table 1 [11].

Decomposing the LMR onto irrps listed in Table 1, we obtain the total number of first non-interacting modes and their symmetries (irrps) at $\boldsymbol{k}=0$. From the reduction formula:

$$a_\mu = \frac{1}{||g||}\sum_\mu \chi^{\mathrm{LMR}}(\{g\}|\tau)\cdot\chi_\mu^*(\{g\}|\tau)\ , \qquad (1)$$

where μ runs over irrps $\Gamma_{1\pm}$, $\Gamma_{2\pm}$, $\Gamma_{3\pm}$, ($\boldsymbol{k}=0$) and $F_{1\pm,\ 2\pm}$, $\Sigma_{1,2}$, $Y_{1,2}$,L_1 ($\boldsymbol{k}\neq 0$), we obtain the number of allowed modes, their symmetries, and their degeneracy's spanned by the LMR. The characters of F, Σ, Y, and L can be found in Ref. [11]. The obtained normal modes spanned by LMR are listed in Table 2.

3. Multiphonon Raman processes in sapphire

The LMR provides the number and symmetries (degeneracy) of possible first order non-interacting modes listed in Table 2. The higher phonon processes arise from mutual interaction between first order phonons. The phonon scattering processes are permitted via deformation potential together with Fröhlich interaction [13]. The deformation potential is assumed to be independent of the phonon $\boldsymbol{k}$ vector. However, in polar materials LO mode is accompanied by electric field which contributes to a long range ($\boldsymbol{k}$-dependent) Fröhlich Hamiltonian.

Table 1
Characters of irreducible representations of D^6_{3d} (at $\boldsymbol{k}=0$) and the reducible Lattice Modes Representation

{g}	E	C_3^+	C_3^-	C''_{21}/τ	C''_{23}/τ	C''_{22}/τ	I	S_6^-	S_6^+	σ_{v1}/τ	σ_{v3}/τ	σ_{v2}/τ
g(CDML)	1	3	5	7.1	9.1	11.1	13	15	17	19.1	21.1	23.1
$\Gamma_{1+}(A_{1g})$	1	1	1	1	1	1	1	1	1	1	1	1
$\Gamma_{2+}(A_{2g})$	1	1	1	−1	−1	−1	1	1	1	−1	−1	−1
$\Gamma_{3+}(E_g)$	2	−1	−1	0	0	0	2	−1	−1	0	0	0
$\Gamma_{1-}(A_{1u})$	1	1	1	1	1	1	−1	−1	−1	−1	−1	−1
$\Gamma_{2-}(A_{2u})$	1	1	1	−1	−1	−1	−1	−1	−1	1	1	1
$\Gamma_{3-}(E_u)$	2	−1	−1	0	0	0	−2	1	1	0	0	0
χ^{LMR} (g)	27	0	0	−1	−1	−1	3	0	0	−1	−1	−1

From Table 2 it follows that there are eighteen $\boldsymbol{k}=0$ soft modes in sapphire. The frequencies of most of them have been determined by means of Raman spectroscopy (RS) Porto et al. [19] and inelastic neutron scattering (INS) [7] and also theoretically calculated within the framework of density functional perturbation theory (Heid et al. [20]). The symmetry assignment of some modes in Al_2O_3 have been also studied by Ossowski et al. [21]. They used the ML [11] tables of irrps which we have applied in decomposition of the LMR for irrps modes. Among the eighteen sapphire phonons there are several first order principal non-interacting Raman active modes (1-RAM). The symmetries of the 1-RAMs are obtained from the decomposition of the symmetrized squares (SQ) of the vector representation $[V\otimes V]_{(2)}=[(A_{2u}\oplus E_u)\otimes(A_{2u}\oplus E_u)]_{(2)}\rightarrow(A_{1g},E_g)$. The frequencies of the $2A_{1g}$ and $5E_g$ modes have been tabulated by several authors [19]. In here we consider the multiphonon Raman processes resulting from two and three phonon scattering processes (combinations and overtones). From Table 2 it is clear that we obtain seven 1-RAMs, $2A_{1g}$ and $5E_g$ (in accordance with Porto [19] and other authors). Raman selection rules are obtained from the Kronecker Products (KPs) of the seven 1-RAM; such as: $A_{1g}\otimes A_{1g}$, $A_{1g}\otimes E_g$, $E_g\otimes E_g$ for two phonon processes and $A_{1g}\otimes A_{1g}\otimes A_{1g}$, $E_g\otimes E_g\otimes E_g$,...,etc. for three phonon processes with A_{1g}:418 cm^{-1} and 645 cm^{-1}; E_g:378, 432, 451, 578 and 751 cm^{-1}. The combinations ($\gamma_1\pm\gamma_2$) and the overtones 2γ are symmetry allowed when the corresponding KP contains one of the 1-RAM. The above selection rules are also valid for modes originating from the entire first Brillouin Zone (BZ) at $\boldsymbol{k}\neq0$. However, in these cases the wave vector selection rules (WVSRs), (phonon momentum conservation) laws govern the respective KP's. For example, interaction of Σ_2 with Σ_2; $\Sigma_2\otimes\Sigma_2$ will result in A_{1g} mode at $\boldsymbol{k}=0$ (the square of identical representation always contains identity rep) and other resulting phonons with $\boldsymbol{k}\neq0$ determined by WVSRs. The frequencies of Σ_2 can be taken from the neutron scattering data [20].

Table 2
Sapphire normal modes obtained by LMR at high symmetry points and lines

Real normal modes	
Γ	$2\Gamma_{1+}\oplus2\Gamma_{1-}\oplus3\Gamma_{2+}\oplus2\Gamma_{2-}\oplus5\Gamma_{3+}\oplus4\Gamma_{3-}$ (ML Notation)
F	$7F_{1+}\oplus8F_{2+}\oplus6F_{1-}\oplus6F_{2-}$
Σ	$13\Sigma_1\oplus14\Sigma_2$
Y	$13Y_1\oplus14Y_2$
L	$27L_1$

Time reversal symmetry influenced modes.
17*A*, 17*T*, 17*P*.

3.1. Three phonon processes: Combinations

There are many other combinations of the type $F_{1+}\otimes F_{2-}\otimes F_{1-}$, or $T_1\otimes T_2\otimes T_3$, ...etc. These will be discussed elsewhere.

4. Experimental

The multiphonon processes have been already and frequently observed. For example in [22–24] (Fig. 3 p253) a possible overtone of E_g (578 cm^{-1}), internal mode of sapphire, is obtained at 1154 cm^{-1}. The spectra have been taken from the sapphire side. In Ref. [23] on Fig. 8, we observe several sapphire (SA) modes combinations at 861, 917, 1155 cm^{-1}. Also in Ref. [24] Fig. 6 are several overtones and combinations seen at 860, 1007 and 1395 cm^{-1}. In here, we have also investigated second and third order Raman processes in GaN/Sapphire by RS. We observe second and third modes centered at 896, 926, 1046, 1210, 1540 cm^{-1}. The band at 1540±12 cm^{-1} might be a combination of E_g (432 cm^{-1})+E_g (451 cm^{-1})+A_{1g} (645 cm^{-1}). The bands present in our spectra (not shown) are in accordance with theoretically derived selection rules.

5. Experimental set up

The samples grown by plasma-assisted molecular beam epitaxy on (0001) sapphire were investigated by means of inelastic light scattering experiment. Raman spectra were recorded using the 514 nm Ar+laser line for excitation and a Jobin Yron single-pass monochromator fillet with an adge filter and a Hamamatsu C7027 thermo-electrically cooled CCd array for detection. The resolution for these spectra was about 0.5 nm at room temperature.

6. Discussion

In Table 3 we list some multiphonon process in corundum. Generally, optical selection rules are governed by wavevector selection rules (quasi-momentum phonon conservation law). Consider scattering process of two phonons from the point F of the BZ. The general wavevector selection rules read: $\alpha\boldsymbol{k}_F+\beta\boldsymbol{k}_F=\boldsymbol{k}_\Gamma+\gamma\boldsymbol{k}_F$, where α, β, and γ are symmetry operators of

Table 3
Multiphonon processes in Al_2O_3

Species	Type	Frequencies
Two phonon processes: overtones		($4\pm cm^{-1}$)
$[\Gamma_{1+}]_2$	$2\Gamma_{1+}(2A_{1g})$	*a*
$[\Gamma_{3+}]_2$	$2\Gamma_{1+}(2A_{1g})$ or $2\Gamma_{3+}(2E_g)$	*a* or *b*
$[F_{1\pm,2\pm}]_2$	$2\Gamma_{1+}(2A_{1g})$ or $2\Gamma_{3+}(2E_g)$ or $2F_{1+}$	*a* or *b*
$[L_1]_2$	$2\Gamma_{1+}(2A_{1g})$ or $2\Gamma_{3+}(2E_g)$ or $2F_{1+}$or $2F_{2+}$	*a* or *b*
$[T_{1,2}]_2$	$2\Gamma_{3+}(2E_g)$	*b*
$[T_3]_2$	$2\Gamma_{1+}(2A_{1g})$	*a*
Two phonon processes: combinations ($\gamma_1 \pm \gamma_2$)		
$\Gamma_{1+}(A_{1g})\otimes\Gamma_{3+}(E_g)$	$A_{1g}\pm E_g \Rightarrow$(418, 615±378 or 432 or 451 or 578 or 751 cm^{-1})	
Selection Rules for Phonon with $\boldsymbol{k}\neq 0$		
$F_{1\pm}\otimes F_{2\pm}$	$\Gamma_{2+}\oplus\Gamma_{3+}(E_g)$ or $F_{1+}\oplus F_{2+}$	
$F_{1+}\otimes F_{1-}$	$\Gamma_{1-}\oplus\Gamma_{3-}$ or $F_{1-}\oplus F_{2-}$	
$F_{2+}\otimes F_{2-}$	$\Gamma_{1-}\oplus\Gamma_{3-}$ or $F_{1-}\oplus F_{2-}$	
$F_{1+}\otimes F_{2-}$	$\Gamma_{2-}\oplus\Gamma_{3-}$ or $F_{1-}\oplus F_{2-}$	
$F_{1-}\otimes F_{2+}$	$\Gamma_{2-}\oplus\Gamma_{3-}$ or $F_{1-}\oplus F_{2-}$	
$T_1\otimes T_1$	$\Gamma_{3+}(E_g)\oplus\Gamma_{1-}\oplus\Gamma_{2-}$	
$T_1\otimes T_2$	$\Gamma_{1+}(A_{1g})\oplus\Gamma_{2+}\oplus\Gamma_{3-}$	
$T_1\otimes T_3$	$\Gamma_{3+}(E_g)\oplus\Gamma_{3-}$	
$T_2\otimes T_3$	$\Gamma_{1+}\oplus\Gamma_{2+}$	
Three phonon proceeses: overtones		
$[\Gamma_{1+}]_3$	$3\Gamma_{1+}(3A_{1g})$	
$[\Gamma_{3+}]_3$	$3\Gamma_{1+}(3A_{1g})$ or 3 Γ_{2+}or $\Gamma_{3+}(3E_g)$	
$[F_{1+}]_3$	$3\Gamma_{1+}(3A_{1g})$ or $3F_{1+}$or $3F_{2+}$	
$[F_{1-}]_3$	$3\Gamma_{1-}$ or $3F_{1-}$ or $3F_{2-}$	
$[F_{2+}]_3$	$3\Gamma_{2+}$or $3F_{1+}$or $3F_{2+}$	
$[F_{2-}]_3$	$3\Gamma_{2-}$ or $3F_{1-}$ or $3F_{2-}$	
$[T_1]_3$	$3T_2$ or $3T_3$	
$[T_2]_3$	$3T_1$ or $3T_3$	
$[T_3]_3$	$3T_3$	

Where $a=2\times418$ cm^{-1} or 2×645 cm^{-1}, $b=2\times378$ cm^{-1} or 2×432 cm^{-1} or 2×51 cm^{-1} or 2×578 cm^{-1} or 2×751 cm^{-1}.

the sapphire space group. This formula shows that the interaction of two F phonons $\boldsymbol{k}\neq 0$ may result in overtone at the point Γ ($2E_g$; measurable by Raman spectroscopy), or in overtone at point F ($2F_{2+}$: not measurable by Raman spectroscopy). Generally, multiphonon processes originating from the entire BZ (excluding point Γ) may produce phonons at point Γ. That is described in Table 3, by $[F_{1+}]_2 \rightarrow 2E_g$ or $2F_{2+}$. However, the overtone of T_3 may yield only $2\gamma(A_{1g})$ (2×318 or 2×645 cm^{-1}) frequency of 2 A_{1g} at zone center phonon. The $\gamma(T_3)$ phonon frequency can be estimated from the neutron scattering experiment. A comprehensive study of LMR and phonon assignment and also multiphonon selection rules in ZnO and GaN can be found in articles [10,14–18,22,25].

7. Conclusion

- The lattice mode for corundum has been explicitly derived yielding the total number of real modes (not TRS influenced) and their symmetries (degeneracies–species) listed in Table 2.
- The effect of TRS has also been investigated (see Appendix). Several phonons; Λ_{1-3}, T_{1-3} and P_{1-3} have been found to be TRS influenced. The degeneracy of these modes doubles. To our best knowledge that is the first time that the effect of TRS on vibrational modes has been indicated. The effect must be taken into account in the interpretation of experimental data obtained by neutron scattering, X-ray and RS with respect to the increase of the dimensions of corresponding dynamical matrices for phonon dispersion curves calculations.
- The selection rules for two and three phonon scattering processes have been investigated. In Table 3 we list symmetry allowed phonons resulting from two and three phonon scattering processes. Their frequencies are explicitly given.
- A comparison of the derived phonon selections rules with available data is made. A good agreement has been found.

Acknowledgement

We would like to thank Ms. L.C. Prinsloo for her experimental assistance.

Appendix A. The Time Reversal effect on Vibrational modes in Al_2O_3

When an irrp is complex, the time reversal symmetry must be taken into account. Using the Frobenius–Schur [12] theorem we have investigated all irrps of corundum. We have found $\Lambda_{1,2,3}$, $T_{1,2,3}$, and $P_{1,2,3}$ irrps complex. Therefore, the modes Λ, T and P are time reversal influenced. The states are classified according to $\Lambda\oplus\Lambda^*$, $T\oplus T^*$, $P\oplus P^*$, respectively. Consequently, the degeneracy of these becomes doubled. In the case of two Λ-Phonons (influenced by TRS), the scattering processes are described by KP $(\Lambda\oplus\Lambda^*)\otimes(\Lambda\oplus\Lambda^*)$. This KP has to be decomposed onto irrps (species) of the resulting in that process. Thus, we have to generate complex representations to deal with the problem. To our best knowledge this is the first-time consideration, which includes the TRS effects in the phonon scattering processes. The physical consequences of the TRS in phonon scattering processes and optical transitions will be considered elsewhere.

References

[1] S. Nakamura, M. Senoh, N. Iwasa, S. Nagahama, T. Yamada, M. Makai, Jpn. J. Appl. Phys. Part 2 34 (1995) L1332.
[2] J.W. Orton, C.T. Foxon, Rep. Prog. Phys. 61 (1998) 1.
[3] O. Weis, J. Phys. (Paris) 33 (1972) C449.
[4] A.G. Every, G.L. Koos, J.P. Wolfe, Phys. Rev., B 29 (1984) 2190.
[5] H. Bialas, O. Weis, H. Wendel, Phys. Lett., A 43 (1973) 97.
[6] H. Bialas, Z. Phys., B 27 (1977) 319.
[7] H. Schrober, D. Strauch, B. Dorner, Z. Phys., B 29 (1993) 273.
[8] M.E. Thomas, R.I. Joseph, W.J. Tropf, Appl. Opt. 27 (1989) 239.
[9] M.E. Thomas, Appl. Opt. 28 (1989) 3277 (10).
[10] H.W. Kunert, Appl. Surf. Sci. 12–213 (2003) 890.
[11] S.C. Miller, W.F. Love, Table of Irreducible Representations of Space Groups and Co-Representations of Magnetic Space Groups, Pruett Press Boulder, Colorado, 1967.
[12] G. Frobenius, I. Schur, Berl. Ber. (1906) 186.
[13] M. Cardona, in: M. Cardona, G. Guntherodt (Eds.), Topics Appl. Phys., vol. 50, Springer, Berlin, 1982, p. 19ff.
[14] H.W. Kunert, Superlattices Microstruct. 36 (2004) 651.
[15] U. Haboeck, H. Siegle, A. Hoffmann, C. Thomsen, Phys. Status Solidi, C *O* 6 (2003) 1710.
[16] J. Birman, Phys. Rev. 131 (1963) 1489.

[17] H.W. Kunert, Cryst. Res. Technol. 38 (2003) 366.
[18] H.W. Kunert, et al., Phys. Status Solidi, C 2 (2005) 1131.
[19] S.P.S. Porto, R.S. Krishnan, J. Chem. 47 (3) (1967) 1009.
[20] H. Schober, D. Strauch, B. Dorner, Z. Phys., B 92 (1993) 273.
[21] M.M. Ossowski, L.L. Boyer, M.J. Mehl, Phys. Rev., B 66 (2002) 22402.
[22] H.W. Kunert, Eur. Phys. J. Appl. 27 (2004) 251.
[23] H.W. Kunert, D. Dale, L.C. Prinsloo, M. Hayes, J. Barnas, J.B. Malherbe, D.J. Brink, A.I. Machatine, K.M. Haile, Eur. Phys. J., Appl. Phys. 27 (2004) 267.
[24] H.W. Kunert, D.J. Brink, M. Hayes, J. Malherbe, L. Prinsloo, J. Barnas, A.G.I. Machatine, M.W. Diale, Phys. Status Solidi, C 1 (2) (2004) 223.
[25] R.P. Wang, Phys. Rev., B 69 (2004) 113303.